Catalysis Today 250 (2015) 60–65

Contents lists available at ScienceDirect

Catalysis Today

journal homepage: www.elsevier.com/locate/cattod

Importance of the sulfidation step in the preparation of highly active $NiMo/SiO_2/Al_2O_3$ hydrodesulfurization catalysts

Aline Villarreal, Jorge Ramírez*, Luis Cedeño Caero, Perla Castillo Villalón, Aída Gutiérrez-Alejandre

UNICAT, Departamento de Ingeniería Química, Facultad de Química, Universidad Nacional Autónoma de México (UNAM), Cd. Universitaria, México D.F., Coyoacán 04510, Mexico

ARTICLE INFO

Article history:
Received 19 November 2013
Received in revised form 8 February 2014
Accepted 17 March 2014
Available online 14 April 2014

Keywords:
HDS
NiMo catalyst
Citric acid
TPS
Silica-alumina

ABSTRACT

The influence of the heating rate on the degree of sulfidation and hydrodesulfurization activity of $NiMo/SiO_2/Al_2O_3$ catalysts prepared with and without citric acid was analyzed. The temperature programmed sulfidation patterns of the catalysts were obtained by following the consumption of H_2S at different rates of heating (1, 3 and 10 K/min). The resulting dispersion of MoS_2 crystallites was observed by transmission electron microscopy, and the reducibility of the different metal species was analyzed by temperature programmed experiments. The results of catalytic activity during the HDS of 4,6-dimethyldibenzothiophene show that the use of a slow rate of heating during sulfidation (1 K/min) can increase twice the activity compared to a fast heating rate (10 K/min). The use of citric acid during catalyst preparation produces smaller MoS_2 crystallites without altering the stacking, and a greater number of promoted sites, detected by FT-IR of adsorbed CO. The temperature programmed reduction of the NiMo catalyst with citric acid showed the formation of a Mo-citrate complex.

1. Introduction

Transition metal sulfides have been widely used as hydrotreating catalysts [1,2]. In recent years, additional interest emerged due to more strict environmental legislation, reducing the amount of sulfur in fuels ([3] and references therein [4]). Hydrodesulfurization catalysts are mostly small crystallites of Mo sulfide promoted with Co or Ni supported on alumina. Many studies have investigated the nature of the active phase in these catalysts [5], and the most widely accepted model is the Co(Ni)—Mo—S model proposed by Topsøe and co-workers [6]. In this model the Ni or Co promotes the active phase enhancing the activity of sites located at the edges of MoS_2. Recently, Topsøe has also reported the existence of new sites with metallic character, called BRIM sites. These BRIM sites, located adjacent to the edges in the basal planes of the MoS_2 crystallites, have the ability to perform hydrogenation reactions [7], the preferred route in hydrodesulfurization (HDS) of sterically hindered dibenzothiophenes [3,7–9]. It has been suggested that the more active BRIM sites exist in MoS_2 crystallites with more than one slab. However, they can also exist in one slab crystallites with only weak interactions with the support [11]. The existence of this active BRIM sites, and the avoidance of non-active species can be achieved by carefully controlling the metal–support interaction [10,11] during catalyst preparation. Several methods have been used to this purpose:

Use of supports different from alumina. The importance of the support in HDS catalysts has been known for a long time [12], and the behavior of supports such as SiO_2 [13,14], MgO ([11,15,16] and references therein), ZrO_2 [17,18], TiO_2 [19], and others, have been investigated extensively. Some supports led to high HDS activities but other properties of the support such as low surface area or poor thermal stability have hindered their use. To overcome these disadvantages the use of mixed supports has been proposed; catalysts prepared with amorphous silica-alumina supports have shown good results in the HDS of 4,6-DMDBT associated to increased acidity and less surface hydroxyls bonded to tetrahedral aluminum [1,10,12,20,21].

Addition of chelating agents has also been proposed as a way to increase the activity of HDS catalysts. Ethylenediaminetetraacetic acid, nitrilotriacetic acid, and citric acid have been used for some time [22,23]. Several works in the literature report that citric acid forms a complex with the promoter, which sulfides then at higher temperatures, facilitating the formation of the promoted Co—Mo—S phase [24–26]. It has been also reported that the amount of sulfided Mo in non-promoted catalysts with high Mo loadings is enhanced

* Corresponding author. Tel.: +52 55 56225349/+52 5622 5366; fax: +52 55 56225366/+525 622 5366.
E-mail addresses: jrs@unam.mx, jrs@servidor.unam.mx (J. Ramírez).

http://dx.doi.org/10.1016/j.cattod.2014.03.035
0920-5861/

with the addition of citric acid, due to an increase of dispersion [27].

Controlling the sulfidation: Since complete sulfidation is a key parameter in the preparation of highly active HDS catalysts [28], the process by which the oxide precursor species transforms into the sulfide phase is crucial to the final activity of the catalyst. In the past, sulfidation at high temperatures was used as a method to break the bonds between Mo oxide species and the support and achieve higher degrees of sulfidation. However, sulfidation at high temperatures produces sintering and loss of active phase surface area, some studies suggest that increasing the sulfidation temperature it is possible to obtain greater number of MoS_2 crystallites with multiple slabs [7]. Further work showed that in order to achieve a higher degree of sulfidation, is convenient to allow the advance of the O—S exchange before reaching 573 K [30]. This result suggests that the heating rate of sulfidation can be an important parameter in the activation of HDS catalysts.

The aim of this work is to determine the effect of the sulfidation rate of heating on the degree of sulfidation, dispersion and catalytic activity of NiMo catalysts supported on silica-coated alumina and post-treated with citric acid. To this end, the reduction patterns of the catalyst precursors and the sulfidation behavior of NiMo catalysts treated with and without citric acid were analyzed in temperature programmed reduction (TPR) and temperature programmed sulfidation (TPS) experiments. The effect of the sulfidation heating rate on the dispersion of MoS_2 crystallites was followed by transmission electron microscopy (TEM) observations, and the activity of the catalyst was evaluated in the HDS of 4,6-dimethyldibenzothiophene.

2. Experimental

2.1. Support and catalyst preparation

To obtain the modified SiO_2/Al_2O_3 support, hereafter SA, commercial γ-alumina (SASOL) was modified with SiO_2 using the following procedure: tetraethylorthosilicate (Aldrich, 98%) was slowly added to a suspension of γ-Al_2O_3 in anhydrous ethanol (Aldrich) in order to obtain the required SiO_2 (6 wt%). The suspension was stirred at boiling temperature during 24 h. After that, the support was filtered under vacuum, dried at 373 K for 24 h and finally calcined at 823 K for 4 h.

Two catalysts with and without citric acid (CA/NiMo and NiMo) were synthesized by pore volume impregnation of Mo and Ni, using aqueous solutions of ammonium heptamolybdate (AHM) (Aldrich) and nickel nitrate (Aldrich) in appropriate amounts to obtain a concentration of 2.8 Mo atoms/nm^2 and Ni/(Mo + Ni) ratio of 0.3. After the impregnation step the catalysts were aged for 4 h, dried at 373 K and calcined at 773 K during 4 h. For the NiMo catalyst, after the procedure described above, the catalyst was impregnated by pore volume with demineralized water, aged, dried and calcined at the same conditions. For the CA/NiMo catalyst, after the procedure described above, the catalyst was impregnated by pore volume with an aqueous solution of citric acid (J. T. Baker), using 1 mol of citric acid per mol of Mo, aged for 4 h and finally dried at 373 K. In this catalyst, the calcination was avoided in order to preserve the citric acid effect during sulfidation, avoiding its decomposition which starts at 445 K [29].

2.2. Characterization and catalytic activity

The temperature programmed reduction (TPR) was performed in 0.25 g of dry catalyst, with a continuous flow of 25 mL/min of a H_2/Ar mixture (70/30) with a heating rate of 10 K/min until 1273 K. The consumption of H_2 was measured using a thermal conductivity detector (TCD). Prior to each measurement the sample was preheated in an inert atmosphere of Argon for 30 min at 373 K.

The temperature programmed sulfidation (TPS) experiments were carried out in 0.25 g of catalyst. The evolution of H_2S was followed with UV–vis spectroscopy (Unicam helios α). The spectrophotometer was operated at fixed wavelength of 200 nm. The TPS patterns were obtained at three rates of heating: 1, 3 and 10 K/min until 673 K, keeping at this temperature for 30 min, with a continuous flow of 10 mL/min of a H_2S/H_2 mix (5/95).

Sulfided catalysts were characterized by TEM using a JEOL 2010 microscope with 1.9 Å point-to-point resolution.

For the HDS reaction tests, the sulfided catalysts where placed in a batch reactor with a solution containing 1000 ppm of S as 4,6-DMDBT, using decane as solvent. After loading the liquid reactant and 0.2 g of the catalyst, hydrogen was introduced to the reactor to achieve 1200 PSI at reaction temperature of 593 K. The analysis of the reaction products was performed with an HP6890 gas chromatograph with a column HP-1 (100 m × 0.25 mm × 0.5 μm).

For infrared spectroscopy, the catalysts were grinded and pressed into self-supporting wafers of about 8 g/cm^2. The prepared wafer was introduced in a double-wall low-temperature infrared transmission cell with KBr windows. The catalyst was sulfided in situ at 673 K using a heating rate of 1 K/min and cooled down to room temperature in the H_2S (15%)/H_2 stream. The sulfided catalyst was then outgassed under vacuum at 723 K for 2 h (5 K/min ramp) and cooled down to room temperature and to ~100 K using liquid nitrogen. A spectrum was obtained at 1 Torr of CO in equilibrium with the sample. The spectra of adsorbed CO were recorded with a Nicolet Magna 760 spectrometer equipped with a DTGS-KBr detector with 4 cm^{-1} resolution. For comparison purposes, the spectra were normalized to 5 mg/cm^2.

3. Results and discussion

3.1. TPR experiments

The temperature programmed reduction (TPR) experiments can provide information about the reducibility of Mo and Ni species in the catalyst prior sulfidation, which also can be correlated with catalytic activity in thiophene HDS [30].

The TPR patterns of NiMo and CA/NiMo (Fig. 1) are very different in shape and intensity. The TPR pattern of NiMo show two peaks at low temperature (504 and 549 K), additionally there is a reduction zone located at 800–1000 K of very low intensity. The first two peaks can be attributed to easily reducible species such as well

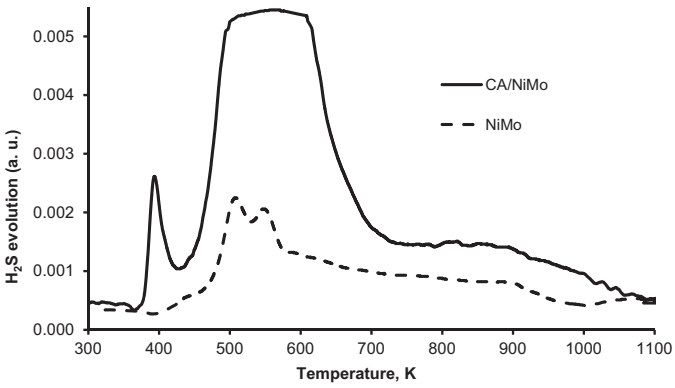

Fig. 1. Temperature programmed reduction patterns for NiMo and CA/NiMo catalysts.

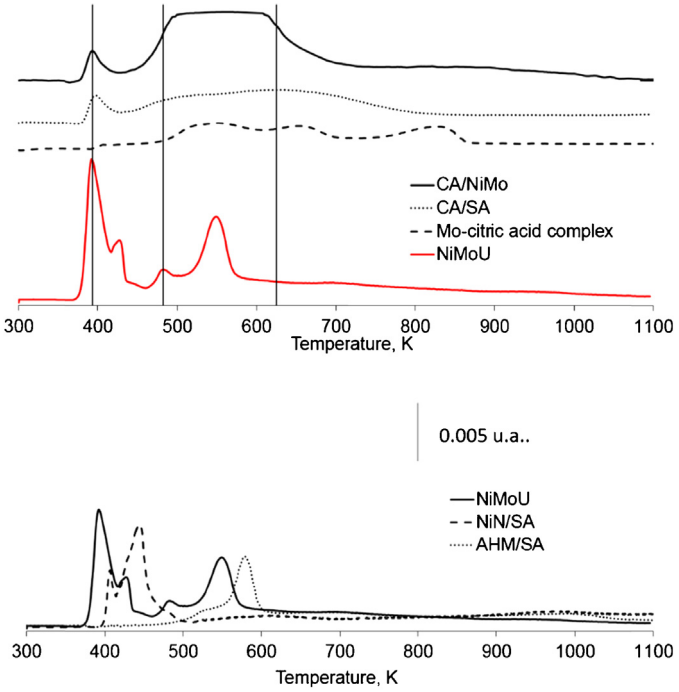

Fig. 2. (a) TPR of: CA/NiMo, CA/SA, unsupported Mo-citric acid complex, and NiMoU. (b) TPR of NiMoU, NiN/SA and AHM/SA.

dispersed octahedral Mo (Oh), and the high temperature peaks are associated to a small quantity of tetrahedral Mo (Td) [19].

In contrast, in the TPR pattern of CA/NiMo, there is only a small contribution of high temperature peaks, and two asymmetrical peaks are present at low temperatures. The amplitude and location of peaks in the TPR are unusual for NiMo catalysts, but taking into account that this catalyst has citric acid and has not been calcined, to assign the different peaks additional TPR experiments were performed on: NiMo uncalcined, supported citric acid, AHM and $Ni(NO_3)_2$ (NiMoU, CA/SA, AHM/SA and NiN/SA) and an unsupported complex of Mo-citric acid.

Fig. 2(a) shows the principal contributions to the TPR pattern of the CA/NiMo catalyst. The peak at 390 K is identical in intensity and width to the one observed in the TPR of supported citric acid, indicating that this peak is associated to the reduction or thermal decomposition of citric acid. The wide signal, for CA/NiMo that starts at 480 K and ends at approximately 625 K, is caused by several contributions. Its amplitude and temperature indicates that the signals are due to the reduction of complexes formed between citric acid and Mo. The TPR of a Mo-citrate complex (1:1 molar ratio) exhibits the same characteristic broad signals, at slightly higher temperatures than the ones observed in the catalyst TPR as a result of complex-support interactions.

The TPR of uncalcined NiMo (Fig. 2(b)) shows four narrow signals. Two signals are attributed to nickel species reduction, one around 400 K and the other around 430 K. For AHM reduction also two signals are observed, one located around 505 and the second at 560 K. The increase in the intensity in the TPR trace of NiMoU, and the shift of this signals to lower temperatures observed for NiMo uncalcined result from the interaction between the species of Ni and Mo when impregnated simultaneously.

According to the TPR experiments, the NiMo catalyst has mainly easily reducible octahedral Mo, whereas CA/NiMo contains polymolybdates, Mo-citrate surface complexes, and Ni species interacting with Mo.

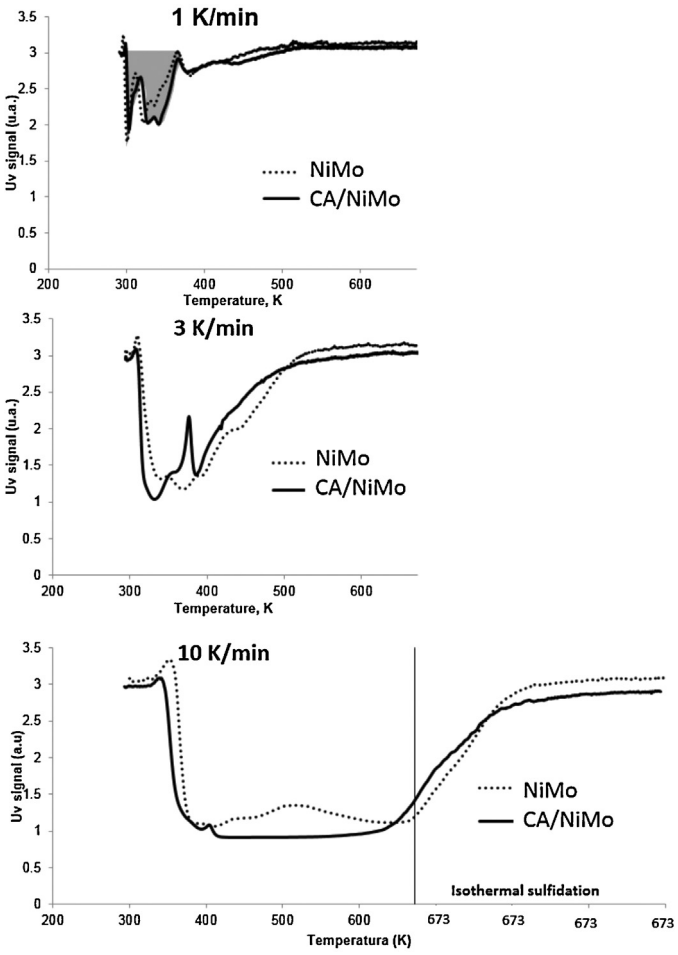

Fig. 3. TPs patterns of the catalyst CA/NiMo (bold line) and NiMo (dotted line) at different heating ramp.

3.2. TPS experiments

The patterns obtained in temperature programmed sulfidation experiments, (shown in Fig. 3) reflect the changes in the sulfidation mechanism caused by the decrease in the heating rate during catalyst sulfidation.

The mechanism of catalyst activation in a H_2S/H_2 atmosphere has not been fully established for supported uncalcined NiMo catalysts modified with citric acid. The sulfidation steps of crystalline MoO_3, first proposed by Moulijn et al. [31], and further confirmed by Weber et al. [32], establishes that at temperatures between 298 and 473 K the species obtained from the sulfidation of MoO_3 with H_2S/H_2 present mainly Mo^{5+} species attributed to oxysulfides, which at higher temperatures reduce to Mo^{4+} consuming H_2 and releasing H_2S. Sulfiding the catalyst with a single heating ramp of 10 K/min from 273 to 673 K, Weber et al. [34], found mostly Mo^{4+} species attributed to MoS_2.

On the contrary, heating the catalyst at 670 K in an inert atmosphere and then contacting with H_2S/H_2 leads mainly to the formation of reduced MoO_2 species with only traces of MoS_2, as reported by Farag et al. [33]. With this procedure the amount of MoS_2 obtained from MoO_3 is temperature dependent and the sulfidation is only complete at high temperature (1073 K). In addition, it was shown that at low temperatures the sulfidation of MoO_3 leads first to oxysulfides and then to MoS_3, which reduces to form the more stable MoS_2 [34].

To facilitate the analysis, the TPS patterns shown in Fig. 3 were divided in two zones of H_2S consumption separated by the last H_2S

production peak. The ratio of the areas of these two zones indicates the amount of sulfided Mo^{6+} compared with that of sulfided Mo^{4+}. For the sake of clarity, the low (gray) and high temperature (white) areas used to calculate the ratio of Mo^{6+}/Mo^{4+} sulfided is shown, for the case of 1 K/min, in Fig. 3.

The ratio of low temperature/high temperature area, shown in Table 1, is almost two for catalysts sulfided at slow rate, 1 and 3 K/min.

In the case of sulfidation at 10 K/min, for the NiMo catalyst the H_2S area related to O—S exchange is marginal compared to the area of the high temperature zone attributed to sulfidation of Mo^{4+}species, giving an area ratio of 0.13. After adding citric acid, CA/NiMo catalyst, the ratio increases to 0.8, indicating an increase in the number of species sulfided in the low temperature region.

This result shows that slow heating during sulfidation allows most of H_2S consumption to take place at low temperatures. As reported in the literature, the H_2S consumption at low temperatures is related to O—S exchange in Mo^{6+} increasing the formation of Mo^{5+}, which at higher temperatures reduces to Mo^{4+} [32].

It is likely that at the low rate of heating during sulfidation most of the Mo species were sulfided by the O—S exchange mechanism, while using a fast rate of heating leaves little time for low temperature H_2S consumption, causing most of the sulfidation to occur in the high temperature zone. The results in the literature indicate that under this conditions poor levels of sulfidation are obtained [33]. This could be because the reduction of Mo occurs first and the sulfidation of a reduced Mo species is difficult.

In general, the temperature at which the TPS trace returns to the baseline, moves to lower temperatures when the heating rate decreases (see Table 1). For the highest heating rate (10 K/min), H_2S consumption stops within the isothermal period at 643 K, while when heating at 3 K/min the catalyst no longer consumes H_2S at 569 K. Finally, at the slowest heating ramp (1 K/min) the baseline return occurs at 522 K, 150 K before the fastest heating ramp.

Using the same heating ramp the sulfidation patterns of catalysts with and without CA show a similar shape, and the temperature at which the TPS trace returns to the base line is similar. The effect of citric acid is best noticed when the heating rate is fast (10 K/min), and minor when the heating ramp during sulfidation is slow (1 K/min).

3.3. Transmission electron microscopy

TEM was used to investigate the stacking and length of the MoS_2 slabs. Fig. 4 shows the slab length distribution for the NiMo catalyst; it is observed that the slab length was modified with the heating ramp during sulfidation. For 1 K/min the average length is 42 Å and for 3 and 10 K/min the slab length is about 44 Å.

The slab length distribution for the CA/NiMo catalyst is shown in Fig. 5. For this catalyst, the average crystallite length for the 1 K/min rate of heating is 30 Å, smaller than the crystallite length for the other two heating ramps (~48 Å), and also smaller compared to the length of slabs of the NiMo catalyst. This higher amount of small crystallites can explain in part the difference in activity between the two catalysts sulfided at 1 K/min, explained in Section 3.4. This

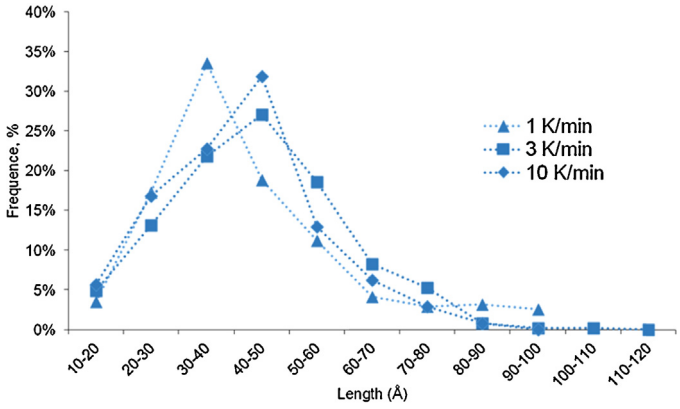

Fig. 4. Slab length distribution NiMo catalyst.

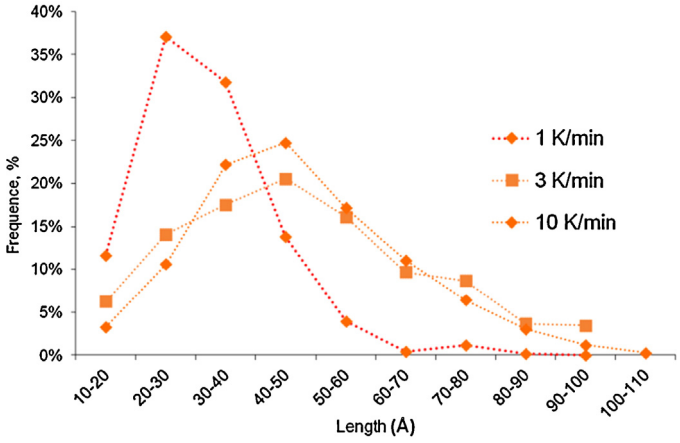

Fig. 5. Slab length distribution CA/NiMo catalyst.

formation of smaller crystallites can be attributed to the formation of a Mo-citric acid complex which isolates Mo as previously reported by Li et al. [25]. Also it is possible that when the CA/NiMo catalyst is sulfided at 1 K/min the complex decomposition is slow preserving the dispersion and preventing agglomeration.

The stacking (Fig. 6) in all the catalysts was mainly of one slab (85–90%). Some crystallites with 2, 3 or 4 layers were observed in all the catalysts; the higher amount of crystallites with 3 or more layers was detected in the CA/NiMo catalyst when the rate of heating was 1 K/min.

3.4. HDS of 4,6-dimethyl dibenzothiophene

The activity of the catalysts was evaluated in the hydrodesulfurization of 4,6-dimethyl dibenzothiophene to quantify the variations due to changes in the sulfidation method.

Fig. 7 shows a comparison of the 4,6-DMDBT HDS pseudo first order constants for NiMo and CA/NiMo. The results show that the effect of the rate of heating during catalyst activation on the HDS

Table 1
Results of TPS and HDS experiments.

Heating rate (K/min)	Ratio low temperature area/high temperature area		Final temperature of H_2S consumption		Selectivity at 50% conversion $\theta = \frac{\text{HYD products}}{\text{DDS products}}$	
	NiMo	CA/NiMo	NiMo (K)	CA/NiMo (K)	NiMo	CA/NiMo
1	1.76	1.98	513	522	8.36	16.68
3	1.75	1.96	584	569	6.50	8.93
10	0.13	0.80	[a]673	[a]673	6.06	8.16

[a] For the heating rate of 10 K/min the H_2S consumption stopped during the isothermal period.

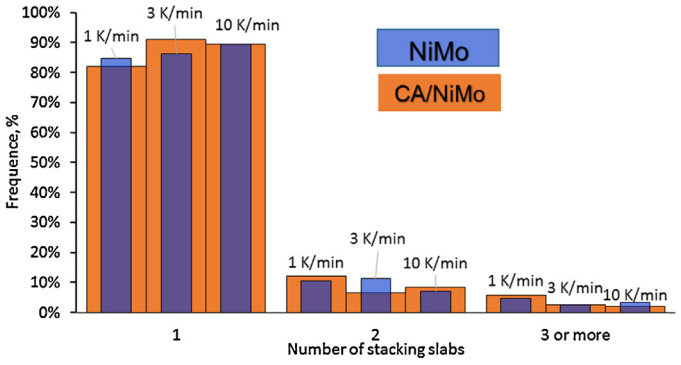

Fig. 6. Stacking distribution.

activity of the catalyst is significant; according to these experiments, sulfiding slowly, using a heating rate of 1 K/min, is possible to double the catalytic activity in both catalysts, with and without citric acid.

These results show the importance of the sulfidation heating ramp. The citric acid addition increases the activity around 30%.

It is known that HDS of 4,6-DMDBT takes place by several parallel reaction routes [20,35,36] the two principals being the direct desulfurization and the hydrogenation. The selectivity, hydrogenation/direct desulfurization, at 50% of conversion (Table 1) indicates that the transformation through the hydrogenation route is enhanced when citric acid is added. As we expected the global HDS activity (Fig. 7) increased when the selectivity towards the hydrogenation route was enhanced.

The selectivity towards the hydrogenation route was higher in the catalyst with citric acid for every sulfidation heating ramp used. The selectivity of CA/NiMo is around 26% bigger than that of NiMo when the catalyst are sulfided at 3 and 10 K/min. The increase could be an effect of citric acid, which produces better sulfided catalyst as showed in the TPS experiments.

In the case of the heating ramp of 1 K/min, the selectivity towards the hydrogenation route in CA/NiMo is twofold that of the catalyst without citric acid. The increase can be related with changes in the promotion level induced by citric acid in the MoS_2 crystallites discussed in the following section.

3.5. IR analysis of adsorbed CO

To study the differences of the actives sites in both catalysts sulfided using a 1 K/min heating ramp, FT-IR experiments of absorbed CO at low temperatures were performed.

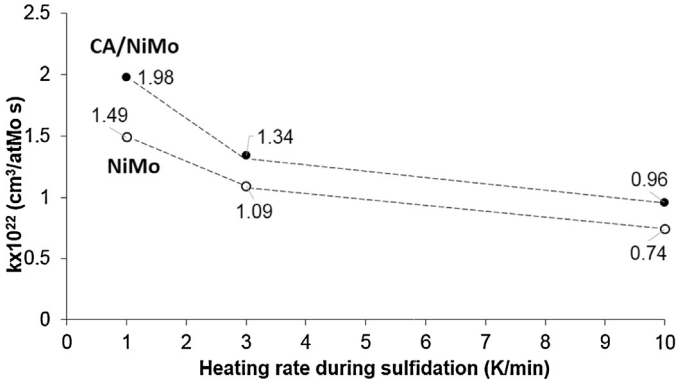

Fig. 7. Pseudo-first order constant ($k \times 10^{22}$ cm^3/at Mo s) for the HDS reaction of 4,6-DMDBT at 593 K and 1200 PSI, for NiMo and CA/NiMo sulfided at different heating rates.

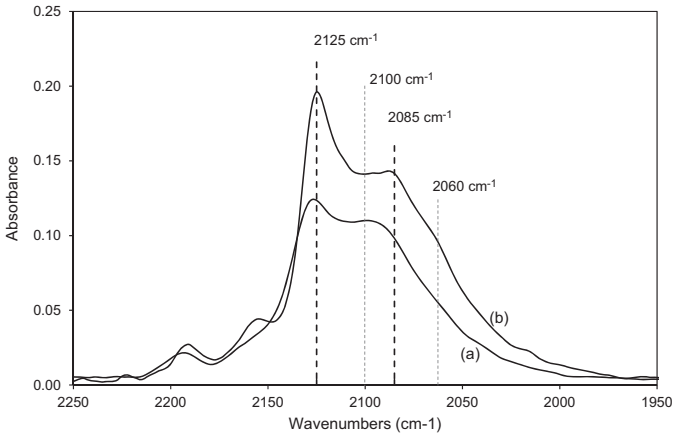

Fig. 8. IR spectra of CO adsorbed on (a) NiMo and (b) CA/NiMo catalyst after sulfidation using a 1 K/min rate of heating.

The FTIR spectra of adsorbed CO on the sulfided catalyst at 100 K and 1 Torr are shown in Fig. 8. According to the literature [37,38], the low intensity bands located at 2191 and 2155 cm^{-1} correspond to CO interacting with the support, the intensity of this bands is higher in the CA/NiMo catalyst indicating a higher support coverage when citric acid is used.

In the spectra of CA/NiMo the ratio of the intensity of the band at 2125 cm^{-1} attributed NiMoS sites and the intensity of the band at 2100 cm^{-1} (unpromoted sites) is higher than the same ratio for NiMo. Also the catalyst with citric acid exhibits one intense band at 2086 cm^{-1} and a very clear shoulder at 2060 cm^{-1}, both of this features are attributed to promoted sites with high and poor S coordination, respectively [38].

On the contrary, the spectra of the catalyst without citric exhibits a very noticeable band at 2100 cm^{-1} related to unpromoted Mo sites. Also the band at 2086 cm^{-1} can only be identified as an asymmetry within the 2100 cm^{-1} broad band. These characteristics show that a better promotion is achieved with the use of citric acid. This can explain the higher selectivity towards the hydrogenation route observed in the catalyst with citric acid shown in Table 1.

However, according to FT-IR of adsorbed CO both catalysts have promoted and unpromoted sites showing that complete promotion is not achieved.

4. Conclusions

The heating ramp during sulfidation is a fundamental parameter in the preparation of NiMo catalysts. The results show that a slow heating ramp doubles the HDS activity of NiMo catalysts supported on SiO_2/Al_2O_3. The catalysts sulfided with a heating ramp of 1 K/min showed the best activity, the highest H_2S consumption during sulfidation and the smaller crystallite size of MoS_2 crystallites. This indicates that a better dispersion and sulfidation is achieved, leading to a higher catalytic activity.

The addition of citric acid during catalysts preparation formed complexes with both Ni and Mo. The higher consumptions of H_2S during sulfidation indicate that a better sulfidation is achieved with citric acid. In the case of the catalyst sulfided at 1 K/min a significant decrease in particle size of MoS_2 crystallites is observed. Accordingly, the catalyst display the better HDS of 4,6-DMDBT activity. The higher selectivity towards the hydrogenation route can be explained by the better promotion of the MoS_2 crystallites.

Acknowledgments

The authors are grateful for the financial support through IN-114112 DGAPA-UNAM project. We thank Iván Puente Lee for TEM work. A.V.M. thanks CONACyT for scholarship grant number 419865.

References

[1] F.E.M.H. Topsoe, B.S. Clausen, Hydrotreating Catalysis: Science and Technology, Springer, Berlin, 1996.
[2] J. Grimblot, Catal. Today 41 (1998) 111.
[3] A. Stanislaus, A. Marafi, M.S. Rana, Catal. Today 153 (2010) 1.
[4] T. Fujikawa, H. Kimura, K. Kiriyama, K. Hagiwara, Catal. Today 111 (2006) 188.
[5] R. Chianelli, J. Catal. 92 (1985) 56.
[6] H. Topsøe, Appl. Catal., A: Gen. 322 (2007) 3.
[7] H. Topsøe, B. Hinnemann, J. Norskov, J. Lauritsen, F. Besenbacher, P. Hansen, G. Hytoft, R. Egeberg, K. Knudsen, Catal. Today 107–108 (2005) 12.
[8] N. Kagami, B. Vogelaar, A. Langeveld, J. Moulijn, Appl. Catal., A: Gen. 293 (2005) 11.
[9] P. Castillo-Villalón, J. Ramirez, R. Castañeda, J. Catal. 294 (2012) 54.
[10] C. Leyva, M. Rana, J. Ancheyta, Catal. Today 130 (2008) 345.
[11] G.M. Dhar, B. Srinivas, M.S. Rana, M. Kumar, S.K. Maity, Catal. Today 86 (2003) 45.
[12] M. Breysse, P. Afanasiev, C. Geantet, M. Vrinat, Catal. Today 86 (2003) 5.
[13] G.P.A.M. Venezia, V. La Parola, G. Deganello, D. Cauzzi, G. Leonardi, Appl. Catal., A: Gen. 229 (2002) 261.
[14] A. Borgna, E.J.M. Hensen, J.A.R. van Veen, J.W. Niemantsverdriet, J. Catal. 221 (2004) 541.
[15] Y. Joshi, P. Ghosh, M. Daage, W. Delgass, J. Catal. 257 (2008) 71.
[16] M. Zdražil, Catal. Today 86 (2003) 151.
[17] K.C. Pratt, J.V. Sanders, V. Christov, J. Catal. 124 (1990) 416.
[18] S.K. Maity, M.S. Rana, B.N. Srinivas, S.K. Bej, G.M. Dhar, T.S.R.P. Rao, J. Mol. Catal. A: Chem. 153 (2000) 121.
[19] J. Ramírez, G. Macías, L. Cedeño, A. Gutiérrez-Alejandre, R. Cuevas, P. Castillo, Catal. Today 98 (2004) 19.
[20] F. Sánchez-Minero, J. Ramírez, A. Gutiérrez-Alejandre, C. Fernández-Vargas, P. Torres-Mancera, R. Cuevas-Garcia, Catal. Today 133–135 (2008) 267.
[21] M. Breysse, C. Geantet, P. Afanasiev, J. Blanchard, M. Vrinat, Catal. Today 130 (2008) 3.
[22] SHELL, EP 0181 035 B1, SHELL, 1986.
[23] M. Rana, J. Ramirez, A. Gutiérrez-Alejandre, J. Ancheyta, L. Cedeño, S. Maity, J. Catal. 246 (2007) 100.
[24] Y. Okamoto, 19th Annu. Saudi–Japan Symp. 1 (2009) 4.
[25] H. Li, M. Li, Y. Chu, F. Liu, H. Nie, Appl. Catal., A: Gen. 403 (2011) 75.
[26] J. Escobar, M.C. Barrera, J.A. de los Reyes, J.A. Toledo, V. Santes, J.A. Colín, J. Mol. Catal. A: Chem. 287 (2008) 33.
[27] N. Rinaldi, K. Al-Dalama, T. Kubota, Y. Okamoto, Appl. Catal., A: Gen. 360 (2009) 130.
[28] D. Wu, J. Zhou, Y. Li, Chem. Eng. Sci. 64 (2009) 198.
[29] D.A. Al-Sammerrai, M.M. Barbooti, Thermochim. Acta 98 (1986) 119.
[30] R. Thomas, E.M. van Oers, V.H.J. de Beer, J. Madema, J.A. Moulijn, J. Catal. 76 (1982) 241.
[31] B. Scheffer, P.J. Mangnus, J.A. Moulijn, J. Catal. 121 (1990) 18.
[32] T. Weber, J.C. Muijsers, J.H.M.C. Van Wolput, C.P.J. Verhagen, J.W. Niemantsverdriet, J. Phys. Chem. 100 (1996) 14144.
[33] H. Farag, Energy Fuels 16 (2002) 944.
[34] J.W. Weber, Th. Muijsers, J.C. Niemantsverdriet, J. Phys. Chem. 99 (1995) 9194.
[35] C. Song, X. Ma, Appl. Catal., B: Environ. 41 (2003) 207.
[36] D. Whitehurst, Catal. Today 45 (1998) 299.
[37] A. Travert, C. Dujardin, F. Maugé, E. Veilly, S. Cristol, J.-F. Paul, E. Payen, J. Phys. Chem. B 110 (2006) 1261.
[38] B.M. Vogelaar, N. Kagami, T.F. van der Zijden, A.D. van Langeveld, S. Eijsbouts, J.A. Moulijn, J. Mol. Catal. A: Chem. 309 (2009) 79.